Magn Reson Mater Phy
DOI 10.1007/s10334-017-0642-z

RESEARCH ARTICLE

Temperature dependence of ^{1}H NMR chemical shifts and its influence on estimated metabolite concentrations

Felizitas C. Wermter[1,2] · Nico Mitschke[1] · Christian Bock[2] · Wolfgang Dreher[1]

Received: 12 April 2017 / Revised: 16 June 2017 / Accepted: 29 June 2017

Abstract
Objectives Temperature dependent chemical shifts of important brain metabolites measured by localised ^{1}H MRS were investigated to test how the use of incorrect prior knowledge on chemical shifts impairs the quantification of metabolite concentrations.
Materials and methods Phantom measurements on solutions containing 11 metabolites were performed on a 7 T scanner between 1 and 43 °C. The temperature dependence of the chemical shift differences was fitted by a linear model. Spectra were simulated for different temperatures and analysed by the AQSES program (jMRUI 5.2) using model functions with chemical shift values for 37 °C.
Results Large differences in the temperature dependence of the chemical shift differences were determined with a maximum slope of about $\pm 7.5 \times 10^{-4}$ ppm/K. For 32–40 °C, only minor quantification errors resulted from using incorrect chemical shifts, with the exception of Cr and PCr. For 1–10 °C considerable quantification errors occurred if the temperature dependence of the chemical shifts was neglected.
Conclusion If ^{1}H MRS measurements are not performed at 37 °C, for which the published chemical shift values have been determined, the temperature dependence of chemical shifts should be considered to avoid systematic quantification errors, particularly for measurements on animal models at lower temperatures.

Keywords NMR spectroscopy · Spectrum analysis · Brain metabolites · Polar organisms

Abbreviations

NAA	*N*-acetylaspartate
Ala	Alanine
GABA	γ-Aminobutyric acid
Asp	Aspartate
AQSES	Automated quantitation of short echo time MRS spectra
CEST	Chemical exchange saturation transfer
Cr	Creatine
DSS	2,2-Dimethyl-2-silapentane-5-sulfonate
FASTMAP	Fast automatic shimming technique by mapping along projections
Gln	Glutamine
Glu	Glutamate
Lac	Lactate
NMR	Nuclear magnetic resonance
m-Ins	myo-inositol
MRS	Magnetic resonance spectroscopy
NA	Number of accumulation
PCr	Phosphocreatine
PRESS	Point resolved spectroscopy sequence
RF	Radio frequency
SW	Spectral width
T_2	Transversal relaxation time constant
Tau	Taurine
TE	Echo time
tCr	Total creatine

Electronic supplementary material The online version of this article (doi:10.1007/s10334-017-0642-z) contains supplementary material, which is available to authorized users.

✉ Wolfgang Dreher
wdreher@uni-bremen.de

[1] Department of Chemistry, in VIVO-MR Group, University Bremen, 28359 Bremen, Germany

[2] Integrative Ecophysiology, Alfred Wegener Institute Helmholtz Centre for Polar and Marine Research, 27570 Bremerhaven, Germany

Journal : Large 10334 | Dispatch : 4-7-2017 | Pages : 12
Article No : 642 | ☐ LE | ☐ TYPESET
MS Code : MRMP-D-17-00046 | ☑ CP | ☑ DISK

TMS	Tetramethylsilane
TR	Repetition time
VAPOR	Variable power and optimised relaxation delays

Introduction

AQ1 In vivo localised ^{1}H NMR spectroscopy (MRS) allows to non-invasively measure numerous metabolites in brain tissue, thus offering the possibility to study characteristic metabolic changes and identify biomarkers of diseases [1–7]. Therefore, a reliable quantification of brain metabolites is essential for the relevance of in vivo MRS. While long echo time (TE) ^{1}H MRS or editing sequences can be good solutions if only a small number of metabolites is of specific interest, short TE ^{1}H MRS is often preferred, because it allows the simultaneous detection of a large number of metabolites and reduces signal losses caused by T_2 relaxation and J-modulation. However, since the analysis of short TE ^{1}H MR spectra of the brain is often hampered by severe signal overlap, the use of prior knowledge on the chemical shifts and the J-coupling constants for all relevant metabolites is of central importance. Thus, well established quantification programs such as LCModel [8], QUEST [9, 10], or AQSES [11] use a model function for each metabolite to minimise the number of variables during the fitting procedure. These model functions are either measured on phantom solutions or simulated using published values of chemical shifts and J-coupling constants as prior knowledge [12, 13]. The similarities and differences between AQSES, which was used in this study, and other quantification methods have been described by Poullet et al. [11].

The extensive use of prior knowledge allows the quantification of 20 or more metabolites, at least for high magnetic field strengths and excellent B_0 homogeneity [5, 14–19]. However, even under favorable experimental conditions and if correct prior knowledge is used, the separate quantification of some metabolites is difficult. For example, glutamate (Glu) and glutamine (Gln), which play an important role in several neurological and psychiatric diseases, often cannot be adequately separated at lower B_0 field so that only their sum (Glx = Glu + Gln) is determined. Similar problems exist for the separate detection of creatine (Cr) and phosphocreatine (PCr), which are important metabolites for the cellular energy status. The concentration of Cr and PCr can considerably change under specific diseases [20]; however, in many cases only the total creatine (tCr = Cr + PCr) signal can be quantified [21].

In addition to the application as a tool for diagnostics and biomedical research, in vivo MRS can also be used to quantitatively evaluate data measured by chemical exchange saturation transfer (CEST) MRI. This signal enhancement technique allows the indirect detection of endogenous or exogenous molecules with exchangeable protons of amide, amine, or hydroxyl groups (for reviews see [22, 23]). Since the size of the observed CEST effect depends on the pool sizes (water, metabolites), an accurate metabolite quantification is of central importance.

In vivo MRS studies on humans and rodents are usually conducted at a basal body temperature of about 37 °C. However, pyrexia or anaesthesia can have a significant impact on body temperature, with changes in body temperature up to about 40 °C or down to 32–35 °C under anaesthesia in rodents, particularly if an external body temperature control system is missing [24].

Recently, the use of alternative animal models for in vivo MR studies in experimental medicine or in comparative physiology have gained increasing interest, including those that use birds [25], lower vertebrates such as amphibians [26], fishes [27], and invertebrates [28]. The body temperatures of these organisms are usually far away from 37 °C or depend on their environmental temperature (ectothermic animals) that can range from very low temperatures around the freezing point of water [29] up to 40 °C and higher in insects [30].

A previous study of Henry et al. [31] used ^{1}H MRS to investigate the brain metabolism of ground squirrels before, during, and after hibernation at temperatures of about 37 and 7 °C. In this article, Henry et al. considered the potential influence of the temperature dependence of chemical shifts and J-coupling constants by using separate basis sets measured at high and low temperature. However, it remained unclear how important the use of separate basis sets for the different temperatures was, i.e. how large the changes in chemical shifts were.

Additional studies have only examined the influence of temperature on the ^{1}H chemical shifts of amide protons [32], proteins [33], and solvents used for reference signals [34–36]. Thus, the present study aims to determine the temperature dependence of ^{1}H chemical shifts of important brain metabolites and to investigate its influence on spectrum quantification if temperature induced changes in chemical shift values are not taken into consideration, i.e., if incorrect prior knowledge is used.

Therefore, in vitro measurements were conducted over a broad temperature range on phantom solutions to examine the influence of temperature changes on the ^{1}H chemical shifts, particularly of those brain metabolites which give rise to CEST effects. Subsequently, simulations were performed to analyse the consequences for spectrum quantification, with special focus on tCr and Glx, and the separate quantification of the contributing metabolites Cr, PCr, Glu, and Gln.

Journal : Large 10334 | Dispatch : 4-7-2017 | Pages : 12
Article No : 642 | ☐ LE | ☐ TYPESET
MS Code : MRMP-D-17-00046 | ☑ CP | ☑ DISK

Materials and methods

Metabolite solutions and experimental localised spectroscopy

All NMR measurements were performed on a 7 T animal scanner (BioSpec 70/20 USR, Bruker BioSpin, Ettlingen, Germany) equipped with a standard B_0 gradient system (BGA-12S2, maximum gradient strength 440 mT m^{-1}, rise times 130 μs). A quadrature birdcage coil (72 mm inner diameter) was used for both RF excitations and signal detection. FASTMAP (Fast Automatic Shimming Technique by Mapping Along Projections) was applied to optimise B_0 homogeneity within the volume of interest [37] ensuring line widths (full width at half maximum) ≤6 Hz.

Localised ^{1}H spectra were acquired using a point resolved spectroscopy sequence (PRESS) [38] consisting of an optimised 90° Shinnar-Le Roux-pulse [39] of 0.6 ms duration, which was calculated by the RF pulse module of the free software suite VESPA (version 0.8, http://scion.duhs.duke.edu/vespa/project), and two 180° Mao4-pulses of 1.75 ms duration [40]. Additionally, the following sequence parameters were used: echo time TE = 7.5 ms, repetition time TR = 15 s, number of accumulations NA = 16, spectral width SW = 4006 Hz, 8192 complex data points, a voxel size 8 × 8 × 8 mm^3, and eddy current compensation using the unsuppressed water signal. The PRESS sequence was preceded by seven RF pulses with variable pulse power and optimised relaxation delays (VAPOR) used for water suppression [3].

For the NMR measurements of important brain metabolites, three or four compounds (each with 10 mM concentration) were dissolved in phosphate buffered saline (12 mM HPO_4^{2-}, 0.1 M NaCl) and titrated to a pH value of 7.0. Finally, 2,2-dimethyl-2-silapentane-5-sulfonate (DSS) was added as chemical shift Ref. [41]. In each group, only such metabolites were combined that do not cause signal overlap in the spectrum. Solution (1): *N*-acetylaspartate (NAA), alanine (Ala), γ-Aminobutyric acid (GABA), myo-inositol (m-Ins). Solution (2): Cr, Gln, lactate (Lac). Solution (3): aspartate (Asp), Glu, PCr, taurine (Tau).

The tubes (Ø20 mm) filled with the metabolite solutions were wrapped with heating tubing connected to a circulation thermostat (Lauda Eco RE 630S, Lauda-Brinkmann, Delran, NJ, USA) for measurements at defined temperatures (1–43 °C). Temperature measurements were performed by a two-point calibrated fibre-optical thermometer (Luxtron 504, Polytec, Waldheim, Germany) inside the tubes (accuracy: ±0.1 °C).

For improved accuracy and estimation of the measurement errors, each solution was measured six times at any given temperature.

Data processing and fitting

Data processing of the metabolites NAA, Ala, GABA, Asp, Cr, PCr, m-Ins, Lac, and Tau was performed using the program ACD/NMR Processor (ACD/Labs, Academic Edition, version 12.01). Data processing consisted of apodisation with a sine function, zero filling to 16 K complex data points, Fourier transformation, and an interactive phase correction. For most metabolites, chemical shifts were determined by direct measurements of the peak positions.

The metabolites Gln and Glu were separately processed because of their complex multiplet structure. Data processing was performed using a program written in the interactive data language IDL (Research Systems, Inc., Boulder, CO, USA) with the same processing parameters as mentioned above. Subsequently, the chemical shift values were determined by a C++ program using a simplex algorithm. This optimisation procedure minimised the difference between the experimental and fitted spectra calculated by the GAMMA NMR library [41] and using the J-coupling constants published in [12, 13] as prior knowledge. Downfield signals were neglected because their in vivo observation is hampered for most metabolites by short T_2, exchange processes with water, and overlapping with other resonances [12, 43].

The AQSES quantification algorithm allows a correction to frequency shifts, but only as a common correction for all resonances of a metabolite [11]. This would cause only minor quantification problems if the temperature dependence of all chemical shifts were identical or at least similar. However, differences in the temperature dependence of chemical shifts could cause an inaccurate quantification as a result of using incorrect prior knowledge. Therefore, the temperature dependence of chemical shift differences between the individual resonances of a metabolite were determined. For all metabolites, the group of hydrogen atoms showing the smallest temperature dependence of its chemical shift with respect to the DSS signal (One-Way ANOVA for repeated measurements; Tukey post-test; GraphPad Prism 5.0, Inc., San Diego, CA, USA) was used as subtrahend. The relation between chemical shift and temperature was determined by linear regression [32, 33].

Simulations and quantifications

The spectra of NAA, Ala, Asp, Cr, PCr, Glu, Gln, Lac, and Tau were simulated using the jMRUI software package 5.2 [44]. A C++ program with the GAMMA NMR library was used for GABA and m-Ins, since the simulation in jMRUI failed due to their large spin systems. As prior knowledge for 37 °C, the chemical shifts and J-coupling constants determined on high resolution NMR spectrometers by Govindaraju et al. and Govind et al. were used [12,

Journal : Large 10334 | Dispatch : 4-7-2017 | Pages : 12
Article No : 642 | ☐ LE | ☐ TYPESET
MS Code : MRMP-D-17-00046 | ☑ CP | ☑ DISK

13]. Exploiting the previously determined linear models, the chemical shifts were adjusted to the individual temperatures. The temperature dependent changes in the J-coupling constants were considered negligible.

Assuming strong J-coupling, spectra were simulated for a symmetric PRESS sequence with TE = 8 ms, 1024 complex data acquisition points, and a sampling interval of 0.25 ms. Four noise-free data sets were designed to determine the influence of temperature changes on spectrum quantification.

Set (1) The brain metabolites NAA (9 mM), Ala (0.65 mM), GABA (1.5 mM), Asp (2 mM), Cr (4 mM), PCr (4.5 mM), Glu (8 mM), Gln (3 mM), m-Ins (6.2 mM), Lac (1.3 mM), and Tau (6 mM) were simulated with a typical in vivo line width of 8 Hz [3]. The metabolite concentrations were adjusted to mimic a rat brain [4, 5, 45]. Data sets were simulated for 40, 37, 35, and 32 °C to analyse the potential influence of pyrexia and experimentally induced cooling.

Set (2) Assuming a fish brain, the following metabolite concentrations were used: NAA (5.4 mM), Ala (0.7 mM), GABA (0.9 mM), Asp (1.1 mM), Cr (3.8 mM), PCr (4.7 mM), Glu (5.8 mM), Gln (1.3 mM), m-Ins (2 mM), Lac (3.7 mM), and Tau (4.6 mM) [46]. The line width was 8 Hz. The assumed temperatures were 10 and 1 °C simulating mean temperatures under boreal and polar conditions.

Set (3) This set includes only the metabolites Cr, PCr, Glu, and Gln assuming the same concentrations and temperatures as in set (1). To evaluate the effects of temperature induced changes in chemical shift for different experimental conditions, simulated line widths were 5 Hz, 8 Hz, and 10 Hz.

Set (4) Same metabolites as in set (3), however, with concentrations and temperatures of set (2).

The temperature dependent spectra were analysed using the time-domain quantification method AQSES [11] as provided by jMRUI 5.2. The basis sets of metabolite profiles were simulated for the upfield range using the chemical shifts and J-coupling constants for 37 °C [12, 13] or the temperature matched chemical shift values for other temperatures. All basis sets were simulated for a constant concentration.

Results

Temperature dependent chemical shifts of brain metabolites

Figure 1 depicts the experimentally determined changes in the chemical shift differences of the metabolite signals as a function of temperature. The corresponding linear fit is displayed as dotted line. In order to ensure better comparability between metabolites, the chemical shift differences were normalised to 0 ppm for 37 °C. The slopes obtained by linear regression are summarised in Table 1.

N-acetylaspartate (NAA) For NAA (Fig. 1a), the chemical shift difference between the signals of the $^{2}CH_3$ and $^{3'}CH_2$ group was almost independent of temperature. In contrast, the chemical shift difference between the ^{2}CH and $^{3'}CH_2$ group increased with increasing temperature with a slope of $+2.5 \times 10^{-4}$ ppm/K. The difference between the $^{3}CH_2$ and $^{3'}CH_2$ group decreased with increasing temperature with a slope of -6.0×10^{-4} ppm/K.

Alanine (Ala) The linear regression for the two signals of Ala (Fig. 1b) yielded in a slope of only $+1.5 \times 10^{-4}$ ppm/K.

γ-Aminobutyric acid (GABA) The distance between the signals $^{2}CH_2$ and $^{3}CH_2$ of GABA (Fig. 1c) did not show any temperature dependent changes, whereas the resonance of the $^{4}CH_2$ group approached the $^{3}CH_2$ signal with decreasing temperature ($+7.3 \times 10^{-4}$ ppm/K).

Aspartate (Asp) For Asp (Fig. 1d) the distance between the $^{3}CH_2$ and ^{2}CH signals did not show a significant temperature dependence. In contrast, the chemical shift difference between the $^{3'}CH_2$ and the ^{2}CH signal decreased with decreasing temperature ($+4.2 \times 10^{-4}$ ppm/K).

Creatine (Cr) and Phosphocreatine (PCr) The signals of Cr and PCr showed a similar tendency (Fig. 1e, f), the chemical shift difference between the $^{2}CH_2$ and the $N(CH_3)$ signal increased with decreasing temperature. The linear regressions yielded a slope of -6.2×10^{-4} and -6.7×10^{-4} ppm/K for Cr and PCr, respectively.

Glutamine (Gln) and Glutamate (Glu) The signals of Gln (Fig. 1g) showed different dependencies on temperature. While the ^{2}CH signal slightly shifted away the $^{3'}CH_2$ group with decreasing temperature (-0.6×10^{-4} ppm/K), the distance of the $^{3}CH_2$, $^{4}CH_2$, and $^{4'}CH_2$ signals to the $^{3'}CH_2$ decreased with decreasing temperature (3.4×10^{-4}, 7.6×10^{-4} and 3.0×10^{-4} ppm/K). While the ^{2}CH, $^{3'}CH_2$ and $^{4}CH_2$ signals of Glu (Fig. 1h) are shifted towards the $^{4'}CH_2$ signal with increasing temperature (-3.5×10^{-4}; -0.4×10^{-4}; -3.4×10^{-4} ppm/K), the distance of the $^{3}CH_2$ signal to the $^{4'}CH_2$ signal changes by $+4.9 \times 10^{-4}$ ppm/K.

Myo-inositol (m-Ins) For m-Ins (Fig. 1i), similar changes of the signal distances of the ^{2}CH and $^{4,6}CH$ protons to the $^{1,3}CH$ signal were observed with an averaged slope of $+3.3 \times 10^{-4}$ ppm/K, whereas the difference between the ^{5}CH signal and the $^{1,3}CH$ signal showed the opposite tendency, with a slope of -3.2×10^{-4} ppm/K.

Lactate (Lac) and Taurine (Tau) The chemical shift differences between the ^{2}CH and the $^{3}CH_3$ signal of Lac (Fig. 1j) and between the $^{2}CH_2$ and the $^{1}CH_2$ signals of Tau (Fig. 1k) showed a similar slope, but with opposite sign ($\mp 3.2 \times 10^{-4}$ ppm/K).

The calculated chemical shifts for the different metabolites and temperatures are shown in table S1 of the

Journal : Large 10334 | Dispatch : 4-7-2017 | Pages : 12
Article No : 642 | ☐ LE | ☐ TYPESET
MS Code : MRMP-D-17-00046 | ☑ CP | ☑ DISK

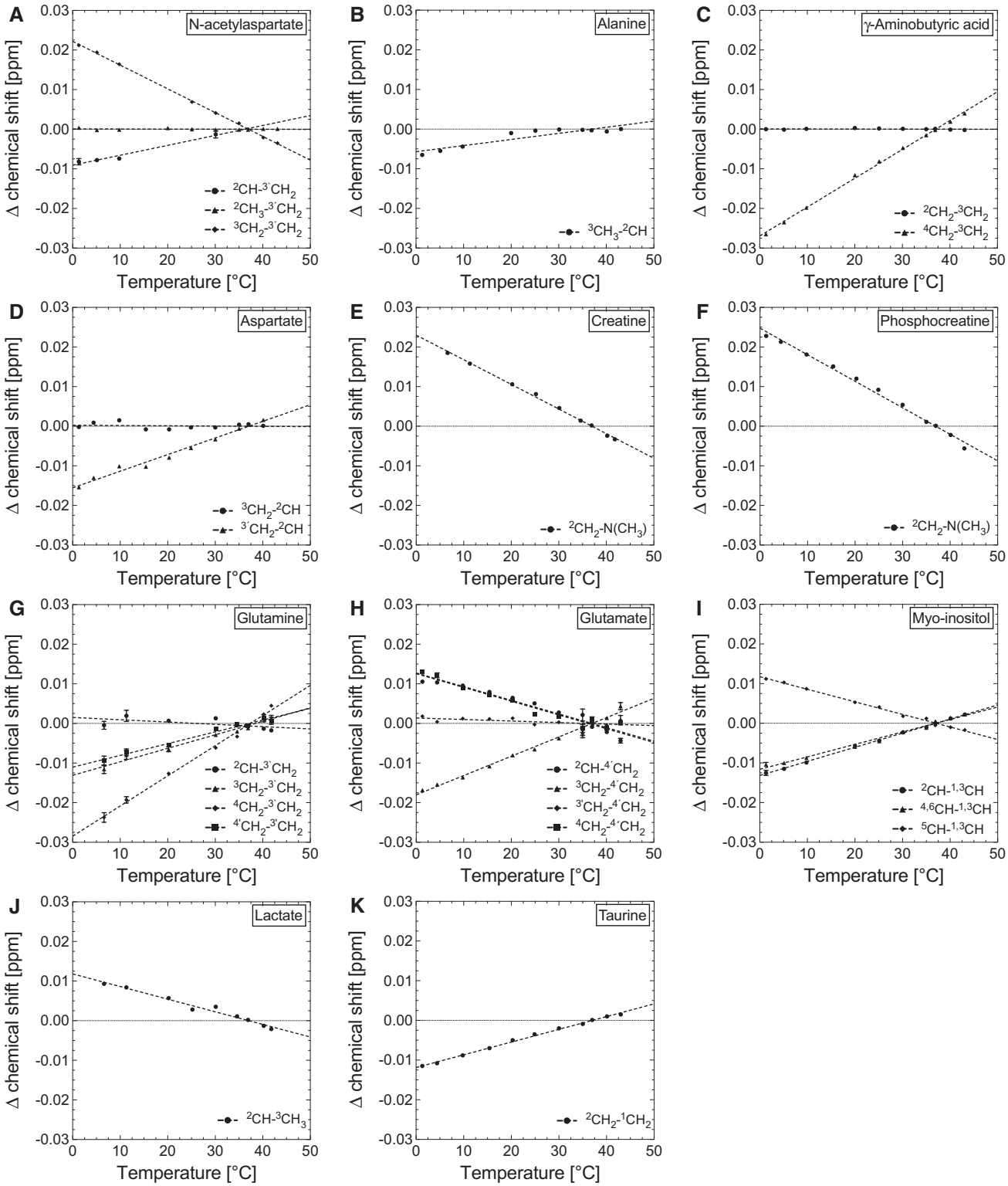

Fig. 1 Experimentally determined chemical shift differences between signals of metabolites (*symbols*) as function of temperature and results of linear regression (*dotted line*)

Journal : Large 10334 | Dispatch : 4-7-2017 | Pages : 12
Article No : 642 | ☐ LE | ☐ TYPESET
MS Code : MRMP-D-17-00046 | ☑ CP | ☑ DISK

Table 1 Slopes resulting from the linear regression of the experimentally determined chemical shift differences between signals of metabolites as function of temperature

Metabolite	Difference	Slope × 10^{-4} [ppm/K]
NAA	^{2}CH-$^{3'}CH_2$	2.5070 ± 0.3126
	$^{2}CH_3$-$^{3'}CH_2$	−0.0234 ± 0.0450
	$^{3}CH_2$-$^{3'}CH_2$	−5.9990 ± 0.0505
Ala	$^{3}CH_3$-^{2}CH	1.5402 ± 0.2368
GABA	$^{2}CH_2$-$^{3}CH_2$	−0.0211 ± 0.0346
	$^{4}CH_2$-$^{3}CH_2$	7.2800 ± 0.1022
Asp	$^{3}CH_2$-^{2}CH	−0.0691 ± 0.1863
	$^{3'}CH_2$-^{2}CH	4.1970 ± 0.1913
Cr	$^{2}CH_2$-$N(CH_3)$	−6.2166 ± 0.1158
PCr	$^{2}CH_2$-$N(CH_3)$	−6.6944 ± 0.1891
Glu	^{2}CH-$^{4'}CH_2$	−3.4740 ± 0.2701
	$^{3}CH_2$-$^{4'}CH_2$	4.8710 ± 0.1684
	$^{3'}CH_2$-$^{4'}CH_2$	−0.3854 ± 0.1853
	$^{4}CH_2$-$^{4'}CH_2$	−3.4450 ± 0.2829
Gln	^{2}CH-$^{3'}CH_2$	−0.5810 ± 0.3044
	$^{3}CH_2$-$^{3'}CH_2$	3.4090 ± 0.2326
	$^{4}CH_2$-$^{3'}CH_2$	7.6150 ± 0.2199
	$^{4'}CH_2$-$^{3'}CH_2$	2.9690 ± 0.1650
m-Ins	^{5}CH-$^{1,3}CH$	−3.1710 ± 0.0725
	$^{4,6}CH$-$^{1,3}CH$	3.1430 ± 0.1217
	^{2}CH-$^{1,3}CH$	3.5590 ± 0.0483
Lac	^{2}CH-$^{3}CH_3$	−3.1866 ± 0.1977
Tau	$^{2}CH_2$-$^{1}CH_2$	3.2098 ± 0.0612

supplementary material. Additionally, the direction of the changes in chemical shifts is illustrated by an arrow.

Quantification of brain metabolites from simulated data sets for different temperatures

Figure 2 illustrates a typical ^{1}H-NMR spectrum with the examined metabolites simulated for 37 °C. The signals are assigned to the metabolites and the corresponding proton groups.

Figure 3 depicts the percentage concentrations determined by the AQSES algorithm for data sets 1 (rat brain) and 2 (fish brain) simulated for the different temperature ranges of 40–32 °C (Fig. 3a) and 10–1 °C (Fig. 3b), respectively, mimicking typical concentrations of the investigated brain metabolites.

For the high temperature range (Fig. 3a), the majority of metabolites showed a maximum variation of 2% from the simulated concentrations. However, large deviations were observed for Cr and PCr, e.g., with an overestimation of Cr by 33% at a temperature of 40 °C. In contrast, the Cr concentration was underestimated by 18% at 35 °C and by 43% at 32 °C. Opposite results were obtained for PCr, yielding an underestimation by 26% at 40 °C and an overestimation at 35 °C (17%) and 32 °C (40%). Additionally, the Asp and GABA concentrations were obviously underestimated and overestimated, especially at 40 °C with 9 and 8%, respectively.

Also, in the low temperature range (Fig. 3b), the concentration of the metabolites Ala, Lac, and Tau were underestimated or overestimated by only 2% or less. NAA and m-Ins showed an underestimation by 4% for 10 °C and by about 6 and 4% at 1 °C, respectively. Furthermore, the concentration of Asp was underestimated by 26% at 10 °C and by 35% at 1 °C. In contrast, the concentration of GABA was overestimated by 14 and 41% at 10 and 1 °C, respectively. In the low temperature range Cr could no longer be quantified. In contrast, PCr was considerably overestimated up to 85%. Glu was slightly overestimated at 10 and 1 °C by about 2%. The metabolite Gln showed an overestimation by about 8% at 1 °C.

Quantification of tCr and Glx from simulated data sets for different temperatures

Figure 4 depicts the quantification results for Cr, PCr, and tCr, as well as Glu, Gln, and Glx (data sets 3 and 4) using the AQSES algorithm again with chemical shift values for 37 °C as prior knowledge. The percentage values with respect to the simulated concentrations are shown for different temperatures and line widths.

For all line widths in the high temperature range, the Cr concentration was overestimated at 40 °C by up to 35%, and maximally underestimated by up to 48% for temperatures lower than 37 °C, while PCr showed the opposite tendency (Fig. 4a, e, i). For data set 4 and temperatures of 10 and 1 °C, a Cr signal was only found for the lowest line width of 5 Hz (Fig. 4b, f, j). However, the tCr signal showed only small deviations for all temperatures and line widths, with a maximum overestimation of about 3% at the lowest temperatures.

For the high temperature range and all line widths (Fig. 4c, g, k), the concentrations of Glu and Gln deviated by about 2%. However, the deviations for the Glx signal are negligible for this temperature range and at line widths of 5–10 Hz. At low temperatures and a line width of 5 Hz, the Glu and the Gln signals were overestimated by up to 10%, whereas at larger line widths for Gln the opposite tendency was observed (Fig. 4d, h, l). In the low temperature range, the concentration of Glx was overestimated by up to 6%.

Discussion

The aim of this study was to investigate systematic quantification errors in vivo ^{1}H MRS caused by ignoring the

Journal : Large 10334 | Dispatch : 4-7-2017 | Pages : 12
Article No : 642 | ☐ LE | ☐ TYPESET
MS Code : MRMP-D-17-00046 | ☑ CP | ☑ DISK

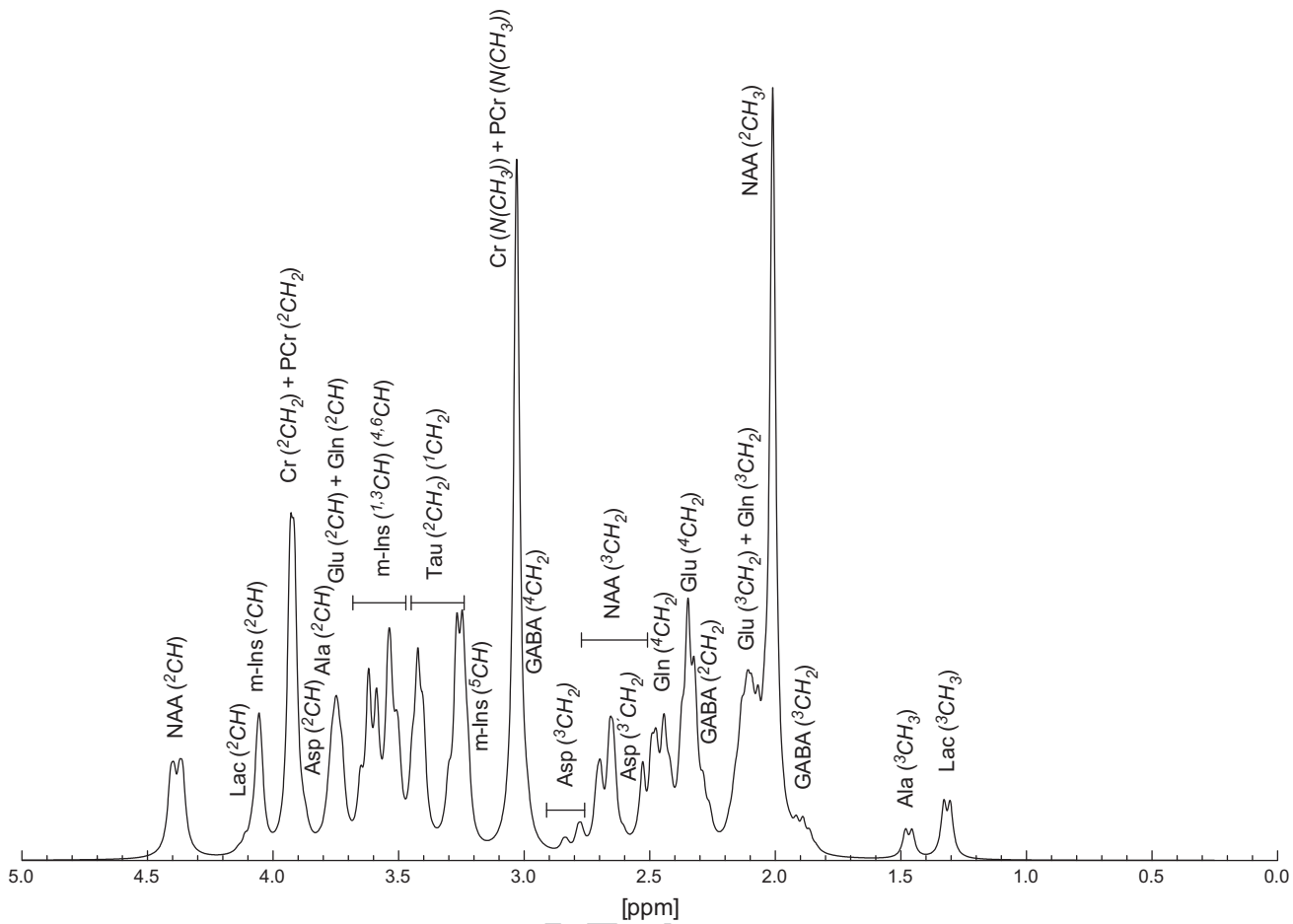

Fig. 2 ^{1}H-NMR spectrum with the examined metabolites simulated for 37 °C and a line width of 8 Hz (*data set* 1)

temperature dependence of ^{1}H NMR chemical shifts in algorithms using prior knowledge. Changes of chemical shifts of important brain metabolites were determined over a wide temperature range of 1–43 °C. Thus, situations caused by illness or experimentally induced temperature changes in mammals as well as animal models with body temperatures far away from 37 °C were considered.

The phantom studies resulted in temperature coefficients in the range between -6.7×10^{-4} and $+7.6 \times 10^{-4}$ ppm/K for the examined metabolites. These changes are of the same magnitude as the average value of -6×10^{-4} ppm/K measured for the established chemical shift reference tetramethylsilane (TMS) published by Hoffman et al. [35]. It is noteworthy that the temperature dependence of the chemical shifts of amide protons is one magnitude stronger as reported by Baxter et al. for proteins [33] and by Arus et al. for NAA [32].

Since even weak temperature dependence can considerably influence quantification results due to the use of incorrect prior knowledge, different data sets were evaluated over a broad temperature range. Special attention was paid to the sum signals tCr and Glx and the possibility to separately quantify Cr and PCr, as well as Glu and Gln. To avoid any influence of noise on the quantification results, noise-free data were simulated. Changes in J-coupling constants with temperature were assumed to be negligible, and only the temperature dependence of the chemical shifts was taken into account. The assumption of negligible changes in J-coupling constants was supported by evaluating the measured multiplets of some metabolites with rather simple multiplet structure as well as a comparison between measured and simulated signals such as Glu (data not shown).

In the high temperature range (32–40 °C), the AQSES algorithm allows an excellent or at least good quantification of the examined metabolites, with the exception of Cr and PCr. While deviations from 37 °C may easily lead to large errors in the concentrations determined for Cr and PCr, the sum signal tCr is almost unaffected if the temperature dependence of the chemical shift values is not taken into account.

Also for the low temperature range (1–10 °C), some metabolites (Ala, Lac and Tau) show only small

Journal : Large 10334 | Dispatch : 4-7-2017 | Pages : 12
Article No : 642 | ☐ LE | ☐ TYPESET
MS Code : MRMP-D-17-00046 | ☑ CP | ☑ DISK

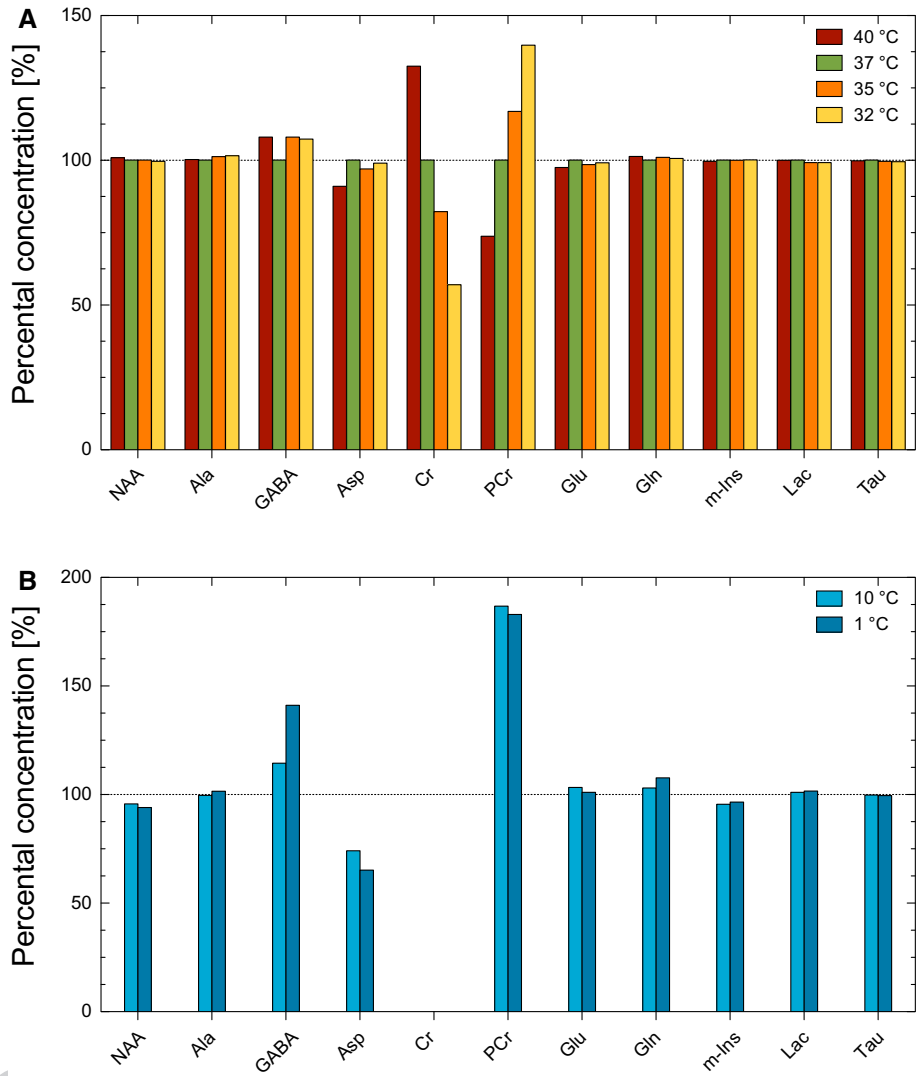

Fig. 3 Metabolite concentrations determined by the AQSES algorithm for data set 1 (**a**) and data set 2 (**b**). The results are given in percent of the simulated values

quantification errors of 2% or less. However, larger quantification errors occur for other metabolites, which are systematically overestimated (GABA, PCr, Glu, Gln) or underestimated (NAA, Asp, Cr, m-Ins) (cf., Fig. 3). It is important to note that the observed specific quantification errors are not only a result of the individual temperature dependence of the chemical shifts, i.e., the use of incorrect prior knowledge for each metabolite. In particular, large errors will occur in case of severe signal overlap, i.e., if the signal of one metabolite can falsely be modelled as signals of other metabolites with changed chemical shift values due to temperature changes.

Thus, the accurate quantification of Ala, Lac, and Tau at all temperatures considered is most likely due to minor overlapping with signals of other metabolites (Fig. 2). However, quantification errors of <8% were found for GABA in the high temperature range, but considerably larger errors occur at lower temperatures. These deviations are caused by increased chemical shift errors at lower temperatures as well as the considerably lower GABA concentration in fish compared to rat brain. Furthermore, there is a considerable signal overlap with signals of other metabolites such as NAA, Cr, PCr, and Glu (Fig. 2). In particular, the overlapping with the $^{4}CH_2$ multiplet of Glu, which is shifted towards to the $^{2}CH_2$ triplet of GABA with decreasing temperature, makes an accurate quantification difficult. Also, the quantification of Asp is hampered in the low temperature range, due to the low concentration and the overlapping of the $^{3}CH_2$ signal of Asp by the dominating $^{3}CH_2$ multiplet of NAA and of the ^{2}CH signal of Asp by the $^{2}CH_2$ singlets of Cr and PCr.

A specific aim of the presented study was to determine the impact of the temperature dependence of chemical shifts on the separate quantification of Glu and Gln, as well as Cr and PCr, and to evaluate the potential errors for the sum signals tCr of Glx. The quantification of Glu and Gln shows deviations from the true values mainly in the low temperature range, with opposite tendencies for Glu and

Journal : Large 10334 | Dispatch : 4-7-2017 | Pages : 12
Article No : 642 | ☐ LE | ☐ TYPESET
MS Code : MRMP-D-17-00046 | ☑ CP | ☑ DISK

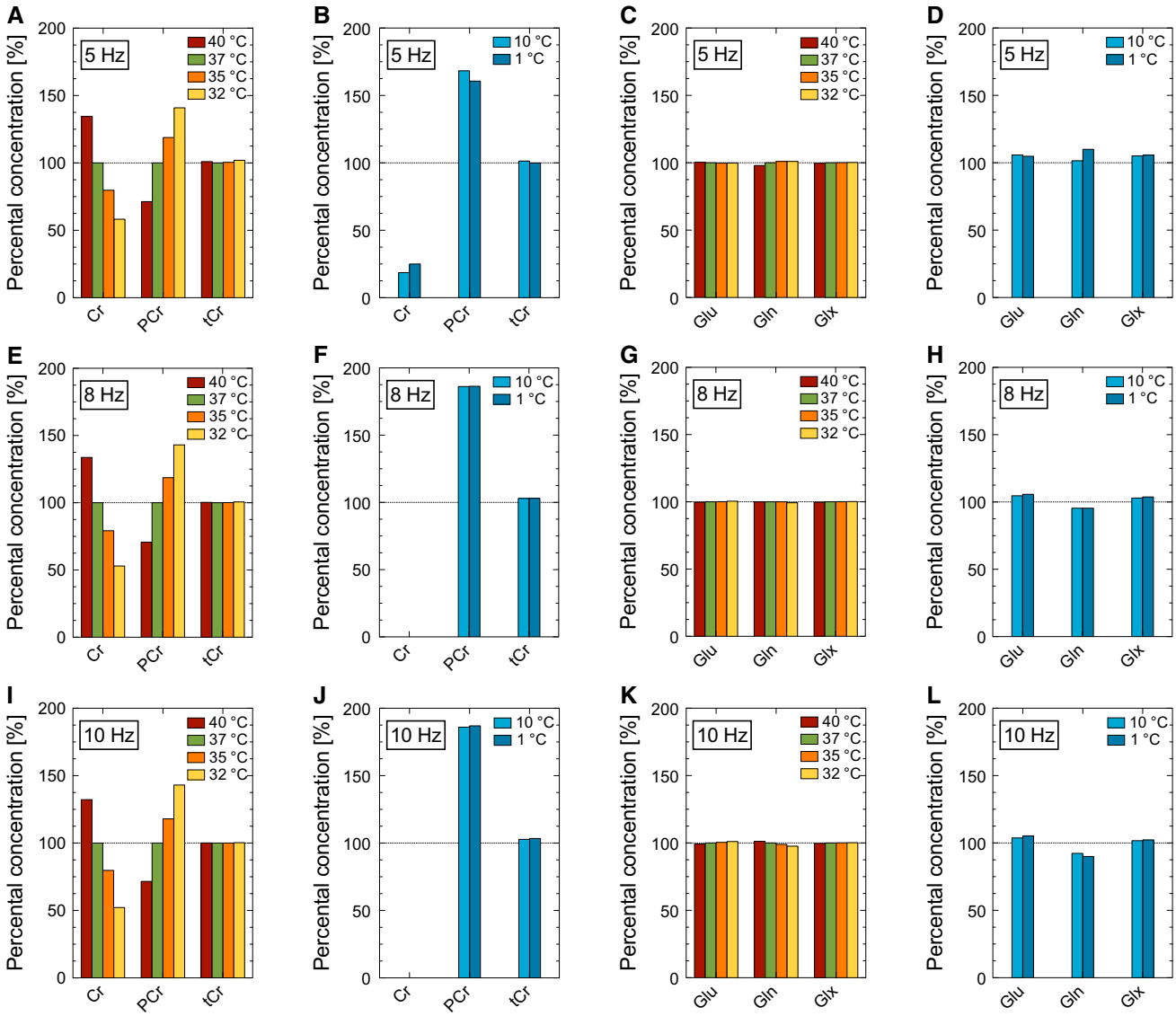

Fig. 4 Metabolite concentrations determined by the AQSES algorithm for Cr, PCr, Glu, Gln and the sum signals tCr and Glx (data sets 3 and 4). The results are given in percent of the simulated values

Gln for a line width of 8 and 10 Hz. The different results for Gln at low temperatures and for a line width of 8 Hz (cf., Figs. 3b, 4h) maybe due to differences in signal overlapping of the ^{2}CH and the $^{3}CH_2$ signal of Gln with signals of other metabolites (cf., Fig. 2). A reason for the rather small deviations in the high temperature range may be the shift of the $^{4}CH_2$ multiplets of Glu and Gln in the same direction (cf., Table 1 and Table S1). Thus, the quantification will not be impeded by additional signal overlapping. It is noteworthy that the Glx signal is quantified with errors of up to 6% for all temperatures and line widths.

The most remarkable result of this study is how large the quantification errors for Cr and PCr are, even for narrow line widths and for small deviations from 37 °C, at which the chemical shift values of the model functions have been determined. Opposite tendencies with respect to under- or overestimation of the concentration are observed for Cr and PCr. The reason seems to be that the signals of the methylene-protons of Cr and PCr shift downfield with decreasing temperature, i.e., the $^{2}CH_2$ signal of Cr shifts with decreasing temperature towards the position of the $^{2}CH_2$ signal of PCr at 37 °C. Thus, at lower temperatures large parts of the Cr signal are quantified as PCr, resulting in an underestimated Cr signal and an overestimated PCr signal, if the basis sets of 37 °C are used. An incorrect quantification of Cr and PCr may easily lead to a misinterpretation of the cellular energetic status. However, the tCr signal showed only minor quantification errors of about 3% for all

Journal : Large 10334 | Dispatch : 4-7-2017 | Pages : 12
Article No : 642 | ☐ LE | ☐ TYPESET
MS Code : MRMP-D-17-00046 | ☑ CP | ☑ DISK

temperatures and line widths, but does not give any information about tissue bioenergetics.

In most cases, the quantification results show the expected influence of line width, i.e., larger deviations for broader line widths. However, a separate quantification of Cr and PCr is hampered independent of line width, even for small temperature changes from 37 °C. While the simulations were performed for 7 T, small changes of chemical shifts due to pyrexia or anaesthesia should also be taken into account at higher B_0 to avoid quantification errors, even in case of an excellent separation between the CH_2 signals of Cr and PCr [16–18]. Alternatively, the CH_3 and CH_2 signals of Cr and PCr could be modelled as separate singlet signals.

It is important to note that the quantification results described in Figs. 3 and 4 also depend on the relative concentrations of metabolites exhibiting overlapping signals. Thus, an increase or decrease by about 0.2 mM of GABA concentration, resulted in a negligible change of the quantification error for 40 °C (data set 1 mimicking rat brain). However, the quantification error for GABA increased by about 5% for a decrease of 0.2 mM and decreased by about 3% for an increase of 0.2 mM at 10 °C (data set 2 mimicking fish brain). Therefore, the reported quantification results describe the general risk of a systematic over- or underestimation of metabolite concentrations when using incorrect prior knowledge. However, the specific numbers will depend on the tissue composition corresponding to the different phantom solutions used in this study.

The quantification errors reported in this study are entirely induced by ignoring the temperature dependence of the chemical shifts and may be further amplified by noise and broader signals under in vivo conditions, particularly for measurements on marine organisms in sea water [47]. Additionally, the presence of more brain metabolites than considered in this study may cause additional spectral overlapping and thus even more severe quantification problems [4].

The presented data show that the temperature dependence of chemical shift values has to be considered to avoid systematic errors caused by using incorrect prior knowledge during spectrum quantification of short TE ^{1}H MRS data. Using the correct chemical shift values as determined in the present study will lead to unbiased data quantification. This was verified for data set 2 (cf. supplementary material). However, the temperature dependence of chemical shifts should also be considered if other MR spectroscopic methods are to be applied at different temperatures, e.g., optimised editing sequences for specific metabolites of interest.

This study focused on the upfield signals of important brain metabolites exhibiting also downfield signals of amine protons, because an accurate quantification based on the upfield signals of these metabolites is essential for evaluating CEST effects [20, 48, 49]. In the future, the temperature dependence of chemical shifts of other brain metabolites has to be studied to build up a complete database for MR quantification of data measured at a certain temperature.

Conclusion

The chemical shift values of upfield signals of important brain metabolites exhibit a temperature dependence that should be taken into account in quantification algorithms that use the chemical shift values as prior knowledge. Ignoring this temperature dependence may cause systematic quantification errors as a result of using incorrect prior knowledge. Minor differences to the usually assumed body temperature of 37 °C in humans or rodents will mainly affect the ability to separately quantify Cr and PCr. However, the temperature dependence of chemical shifts will be of considerable importance for the quantification of MRS data measured at lower temperatures on organisms such as fishes.

Acknowledgements We thank Dr. Peter Erhard for helpful comments on the manuscript. This work was supported by the Deutsche Forschungsgemeinschaft (DFG) in the framework of the priority programme 'Antarctic Research with comparative investigations in Arctic ice areas' (SPP 1158) by grants DR298/13-1 and BO2467/4-1.

References

1. Howe FA, Maxwell RJ, Saunders DE, Brown MM, Griffiths JR (1993) Proton spectroscopy in vivo. Magn Reson Q 9:31–59
2. Ross B, Michaelis T (1994) Clinical applications of magnetic resonance spectroscopy. Magn Reson Q 10:191–247
3. Tkáč I, Starcuk Z, Choi IY, Gruetter R (1999) In vivo ^{1}H NMR spectroscopy of rat brain at 1 ms echo time. Magn Reson Med 41:649–656
4. Pfeuffer J, Tkáč I, Provencher SW, Gruetter R (1999) Toward an in vivo neurochemical profile: quantification of 18 metabolites in short-echo-time ^{1}H NMR spectra of the rat brain. J Magn Reson 141:104–120
5. Mlynárik V, Cudalbu C, Xin L, Gruetter R (2008) ^{1}H NMR spectroscopy of rat brain in vivo at 14.1Tesla: improvements in quantification of the neurochemical profile. J Magn Reson 194:163–168
6. Tkáč I, Oz G, Adriany G, Uğurbil K, Gruetter R (2009) In vivo ^{1}H NMR spectroscopy of the human brain at high magnetic fields: metabolite quantification at 4T vs. 7T. Magn Reson Med 62:868–879
7. Marjańska M, Auerbach EJ, Valabrègue R, Van de Moortele PF, Adriany G, Garwood M (2012) Localized 1H NMR spectroscopy in different regions of human brain in vivo at 7 T: T2 relaxation times and concentrations of cerebral metabolites. NMR Biomed 25:332–339

Journal : Large 10334 | Dispatch : 4-7-2017 | Pages : 12
Article No : 642 | ☐ LE | ☐ TYPESET
MS Code : MRMP-D-17-00046 | ☑ CP | ☑ DISK

8. Provencher SW (1993) Estimation of metabolite concentrations from localized in vivo proton NMR spectra. Magn Reson Med 30:672–679
9. Ratiney H, Coenradie Y, Cavassila S, van Ormondt D, Graveron-Demilly D (2004) Time-domain quantitation of ^{1}H short echo-time signals: background accommodation. Magn Reson Mater Phy 16:284–296
10. Ratiney H, Sdika M, Coenradie Y, Cavassila S, van Ormondt D, Graveron-Demilly D (2005) Time-domain semi-parametric estimation based on a metabolite basis set. NMR Biomed 18:1–13
11. Poullet JB, Sima DM, Simonetti AW, De Neuter B, Vanhamme L, Lemmerling P, Van Huffel S (2007) An automated quantitation of short echo time MRS spectra in an open source software environment: AQSES. NMR Biomed 20:493–504
12. Govindaraju V, Young K, Maudsley AA (2000) Proton NMR chemical shifts and coupling constants for brain metabolites. NMR Biomed 13:129–153
13. Govind V, Young K, Maudsley AA (2015) Corrigendum: proton NMR chemical shifts and coupling constants for brain metabolites. Govindaraju V, Young K, Maudsley AA, NMR Biomed. 2000; 13: 129–153. NMR Biomed 28:923–924
14. Deelchand DK, Van de Moortele PF, Adriany G, Iltis I, Andersen P, Strupp JP, Vaughan JT, Uğurbil K, Henry PG (2010) In vivo ^{1}H NMR spectroscopy of the human brain at 9.4 T: initial results. J Magn Reson 206:74–80
15. Hong ST, Balla DZ, Pohmann R (2011) Determination of regional variations and reproducibility in in vivo ^{1}H NMR spectroscopy of the rat brain at 16.4 T. Magn Reson Med 66:11–17
16. Duarte JM, Lei H, Mlynárik V, Gruetter R (2012) The neurochemical profile quantified by in vivo ^{1}H NMR spectroscopy. Neuroimage 61:342–362
17. Hong ST, Pohmann R (2013) Quantification issues of in vivo ^{1}H NMR spectroscopy of the rat brain investigated at 16.4 T. NMR Biomed 26:74–82
18. Chadzynski GL, Pohmann R, Shajan G, Kolb R, Bisdas S, Klose U, Scheffler K (2015) In vivo proton magnetic resonance spectroscopic imaging of the healthy human brain at 9.4 T: initial experience. Magn Reson Mater Phy A 28:239–249
19. Xin L, Tkáč I (2016) A practical guide to in vivo proton magnetic resonance spectroscopy at high magnetic fields. Anal Biochem. doi:10.1016/j.ab.2016.10.019
20. Cai K, Singh A, Poptani H, Li W, Yang S, Lu Y, Hariharan H, Zhou XJ, Reddy R (2015) CEST signal at 2 ppm (CEST@2 ppm) from Z-spectral fitting correlates with creatine distribution in brain tumor. NMR Biomed 28:1–8
21. Kogan F, Haris M, Singh A, Cai K, Debrosse C, Nanga RP, Hariharan H, Reddy R (2014) Method for high-resolution imaging of creatine in vivo using chemical exchange saturation transfer. Magn Reson Med 71:164–172
22. van Zijl PC, Yadav NN (2011) Chemical exchange saturation transfer (CEST): what is in a name and what isn't? Magn Reson Med 65:927–948
23. Zaiss M, Bachert P (2013) Chemical exchange saturation transfer (CEST) and MR Z-spectroscopy in vivo: a review of theoretical approaches and methods. Phys Med Biol 58:R221–R269
24. Kiyatkin EA, Brown PL (2005) Brain and body temperature homeostasis during sodium pentobarbital anesthesia with and without body warming in rats. Physiol Behav 84:563–570
25. Van der Linden A, Van Meir V, Tindemans I, Verhoye M, Balthazart J (2004) Applications of manganese-enhanced magnetic resonance imaging (MEMRI) to image brain plasticity in song birds. NMR Biomed 17:602–612
26. Stecyk JA, Bock C, Overgaard J, Wang T, Farrar AP, Pörtner HO (2009) Correlation of cardiac performance with cellular energetic components in the oxygen-deprived turtle heart. Am J Physiol Regul Integr Comp Physiol 297:R756–R768
27. Van der Linden A, Verhoye M, Pörtner HO, Bock C (2004) The strengths of in vivo magnetic resonance imaging (MRI) to study environmental adaptational physiology in fish. Magn Reson Mater Phy 17:236–248
28. Melzner F, Bock C, Pörtner HO (2006) Critical temperatures in the cephalopod *Sepia officinalis* investigated using in vivo ^{31}P NMR spectroscopy. J Exp Biol 209:891–906
29. Bock C, Sartoris FJ, Pörtner HO (2002) In vivo MR spectroscopy and MR imaging on non-anaesthetized marine fish: techniques and first results. Magn Reson Imaging 20:165–172
30. Heinrich B (1974) Thermoregulation in endothermic insects. Science 185:747–756
31. Henry PG, Russeth KP, Tkac I, Drewes LR, Andrews MT, Gruetter R (2007) Brain energy metabolism and neurotransmission at near-freezing temperatures: in vivo ^{1}H MRS study of hibernating mammal. J Neurochem 101:1505–1515
32. Arús C, Chang Y-C, Barany M (1985) *N*-acetylaspartate as an intrinsic thermometer for ^{1}H NMR of brain slices. J Magn Reson (1969) 63:376–379
33. Baxter NJ, Williamson MP (1997) Temperature dependence of ^{1}H chemical shifts in proteins. J Biomol NMR 9:359–369
34. Gottlieb HE, Kotlyar V, Nudelman A (1997) NMR chemical shifts of common laboratory solvents as trace impurities. J Org Chem 62:7512–7515
35. Hoffman RE, Becker ED (2005) Temperature dependence of the ^{1}H chemical shift of tetramethylsilane in chloroform, methanol, and dimethylsulfoxide. J Magn Reson 176:87–98
36. Hoffman RE (2006) Standardization of chemical shifts of TMS and solvent signals in NMR solvents. 44:606–616
37. Gruetter R (1993) Automatic, localized in vivo adjustment of all first- and second-order shim coils. Magn Reson Med 29:804–811
38. Bottomley PA (1987) Spatial localization in NMR spectroscopy in vivo. Ann N Y Acad Sci 508:333–348
39. Shinnar M, Bolinger L, Leigh JS (1989) The synthesis of soft pulses with a specified frequency response. Magn Reson Med 12:88–92
40. Mao J, Mareci TH, Andrew ER (1988) Experimental study of optimal selective 180° radiofrequency pulses. J Magn Reson (1969) 79:1–10
41. Wishart DS, Bigam CG, Yao J, Abildgaard F, Dyson HJ, Oldfield E, Markley JL, Sykes BD (1995) ^{1}H, ^{13}C and ^{15}N chemical shift referencing in biomolecular NMR. J Biomol NMR 6:135–140
42. Smith SA, Levante TO, Meier BH, Ernst RR (1994) Computer simulations in magnetic resonance. An object-oriented programming approach. J Magn Reson A 106:75–105
43. Vermathen P, Govindaraju V, Matson GB, Maudsley AA (1999) Detection of downfield ^{1}H resonances in human brain using single voxel and SI methods. In: Proceeding of the 7th scientific meeting and exhibition, International Society for Magnetic Resonance in medicine, Pennsylvania, p 1584
44. Stefan D, Cesare FD, Andrasescu A, Popa E, Lazariev A, Vescovo E, Strbak O, Williams S, Starcuk Z, Cabanas M, van Ormondt D, Graveron-Demilly D (2009) Quantitation of magnetic resonance spectroscopy signals: the jMRUI software package. Meas Sci Technol 20:104035
45. Hong ST, Balla DZ, Shajan G, Choi C, Uğurbil K, Pohmann R (2011) Enhanced neurochemical profile of the rat brain using in vivo ^{1}H NMR spectroscopy at 16.4 T. Magn Reson Med 65:28–34
46. Kabli S, Spaink HP, De Groot HJ, Alia A (2009) In vivo metabolite profile of adult zebrafish brain obtained by high-resolution localized magnetic resonance spectroscopy. J Magn Reson Imaging 29:275–281

Journal : Large 10334 | Dispatch : 4-7-2017 | Pages : 12
Article No : 642 | ☐ LE | ☐ TYPESET
MS Code : MRMP-D-17-00046 | ☑ CP | ☑ DISK

47. Kugel H (1991) Improving the signal-to-noise ratio of NMR signals by reduction of inductive losses. J Magn Reson (1969) 91:179–185
48. Cai K, Haris M, Singh A, Kogan F, Greenberg JH, Hariharan H, Detre JA, Reddy R (2012) Magnetic resonance imaging of glutamate. Nat Med 18:302–306
49. Wermter FC, Bock C, Dreher W (2015) Investigating GluCEST and its specificity for pH mapping at low temperatures. NMR Biomed 28:1507–1517

Journal : Large 10334 | Dispatch : 4-7-2017 | Pages : 12
Article No : 642 | ☐ LE | ☐ TYPESET
MS Code : MRMP-D-17-00046 | ☑ CP | ☑ DISK

Journal:	**10334**
Article:	**642**

Springer
the language of science

Author Query Form

Please ensure you fill out your response to the queries raised below and return this form along with your corrections

Dear Author

During the process of typesetting your article, the following queries have arisen. Please check your typeset proof carefully against the queries listed below and mark the necessary changes either directly on the proof/online grid or in the 'Author's response' area provided below

Query	Details Required	Author's Response
AQ1	Please provide ethical standards and conflict of interest.	